ResearchGate

See discussions, stats, and author profiles for this publication at: https://www.researchgate.net/publication/370923332

Vertical Ground Deformation Monitoring of the Sinabung Volcano in 2021-2022 using Sentinel-1 and DInSAR

Conference Paper · May 2023

CITATIONS
0

READS
188

2 authors:

Hanif Muhammad
Khon Kaen University
22 PUBLICATIONS **141** CITATIONS
SEE PROFILE

Sarun Apichontrakul
Khon Kaen University
1 PUBLICATION **0** CITATIONS
SEE PROFILE

All content following this page was uploaded by Hanif Muhammad on 20 May 2023.

The user has requested enhancement of the downloaded file.

Vertical Ground Deformation Monitoring of the Sinabung Volcano in 2021-2022 using Sentinel-1 and DInSAR

Muhammad Hanif[1], Sarun Apichontrakul[2]*

[1]Graduate Student Geoinformatics, Department of Computer Science, College of Computing, Khon Kaen University; [2] Lecturer of Geoinformatics, Department of Computer Science, College of Computing, Khon Kaen University;*
[*]Phone : 043-009700, E-mail : sarunap@kku.ac.th

ABSTRACT

Mount Sinabung had been dormant for 400 years, but it erupted again in 2010 and has become active since. The objective of this research was to monitor and to analyze monthly vertical ground deformation around Sinabung volcano from 2021 to the end of 2022, and to produce time-series maps of the area to detect deformation trends. This research utilized remote sensing technology and geographical information system (GIS), specifically, Sentinel 1 data and Differential Interferometric Synthetic Aperture Radar (DInSAR) technique. Results of this research showed significant movement of the ground surface and changes in spatial distribution of the volcano area. Some areas deflated, while others inflated. The observed deformation statistics fluctuated from months to months with no significant pattern. The results showed that most of the area around the volcano has been inflated (4,098.33 Ha). The range of deformation measured was between -0.010 to +0.099 meters, with the average of +0.055 meter. In March 2021, there were a total of 13 explosive eruptions, producing ash cloud as high as 5,000 m. Incidentally, inflations of about 0.038 m were observed around the volcano a couple months prior. There were 26 eruptions in April 2021, with the biggest eruption produced ash cloud of 1600 m. From April to August 2021, the deformation ranged around -0.01 to 0.01 meters. After another eruption in August 2021 with ash cloud height of 4,500 m, the deformation was continued to experienced inflation of about 0.038 m. There was a drastic inflation in October which reached 0.033 m, then deflate dramatically to -0.037 m in November 2022. This indicated tectonic activity around the volcano, which was caused by continuous changes in magma pressure underneath, signifying that the volcano is still very active.

Keywords: interferometry; image processing; synthetic aperture radar; deformation; geohazard

INTRODUCTION

Indonesia is an archipelagic country situated on the Ring of Fire. Sumatra island has one of the highest volcanic activity levels on earth and is home to many active volcanoes. The Sinabung volcano is a part of the Toba volcano system, formed around 74,000 years ago. Sinabung had been dormant for 400 years, but it erupted again in 2010 and has become active since [1]. The rate of activity increases because plate motion and changes in Earth's gravity cause pressure anomalies at the base of the mountain (magma chamber). The promotion of local seismic activity on Sinabung Volcano, which results in ground deformation, is a change in an object's shape and dimensions, creating a new geomorphological landscape [1]. The report data from the center of volcanology and mitigation geology hazard showed that the Sinabung volcano has more activities than other volcanoes in Indonesia. There had been 984 eruptions from 2016 to 2021 [2], impacting the area's environment. A big eruption in March 2021 damaged the agriculture area of around 2,945.8 Ha, resulting in economic loss of 1,917,093.42 USD [3]. One of the effects of this volcanism is strain deformation of land surface [4]. The deformation is usually caused by pressure of magma energy and tectonic movement. Monitoring volcanic activity is crucial to mitigate volcanic disasters before the they occur [5][6]. At the moment, the Indonesian government has only one station for monitoring Sinabung's activities, and the recoded data is very limited. Remote sensing data from Sentinel 1 satellite is a very useful alternative observation tool. By using interferometric analysis, the volcanic activities of the whole area can be monitored [7]. The aim of this research was to monitor and to analyze monthly vertical deformation patterns of land surface around Sinabung volcano from 2021 to the end of 2022, to produce time-series maps of the area to detect deformation trends.

METHODOLOGY

The study location is Sinabung volcano in Karo District, North Sumatra Province, Indonesia. This study utilized Synthetic Aperture Radar (SAR) data from the Sentinel 1, obtained from ESA's Copernicus website. The data used was the Sentinel 1 A's C-band wave length of 5.5 cm at incidence angle range of 20º-46º, descending orbit, SLC polarization VV-VH, and beam IW Schwad of 250 km. This analysis used 24 months of data between 2021-2022. Historical volcanic activity data were obtained from the Ministry of Energy and Mineral Resources of

Indonesia. The analysis tool used was the open-source SNAP software. Interferometric analysis techniques has two stage the first is pre-processing data and the second is processing data.

Pre-processing data

The first step was to perform terrain observation with progressive scans SAR or TOPSAR co-registration data processing, which consists of the following steps; import, TOPSAR split, subways, polarization, brush, geometric registration, and spectral diversity enhancement [8]. At this stage, two master data will be combined then produced multi-layer data for the next analysis.

Processing data

This process used the output of TOPSAR co-registration data for DInSAR analysis. This technique compared two phases of two satellite images from different months to determine the deformation changes that had occurred [9]. The initial output of interferometry is the phase value between 0 and 2, which was then transformed into displacement in the meter unit [10]. The result of this analysis is the map of ground deformation between 2021-2022.

Interferogram analysis is used to gain information on the height of the ground surface in a pixel-based. The Differential Interferometric Synthetic Aperture Radar (DinSAR) this technique has been shown to monitor volcanic activity, land subsidence, landslides, and tectonic activities, including analyzing its volume. The results of this analysis are within millimeter precision [10]. DInSAR process includes the pre-processing steps (interferogram formation, net topographic effects, filtering, and multi-search), data unwarping process, and displacement analysis process. This technique measures the relative motion of the scene between two InSAR observations by using the information contained in the second phase SAR imagery to measure the shift between the two pixels [12]. In interferometric analysis, several main stages of data processing must be carried out [13]. At least in observing ground deformation, we use two data records. This technique detects two different phases of interferometry, which contains information from topographical profiles, differences in orbital paths, deformations, and phase noise. The equation can be written as followed [10]:

$$\phi_1 = 4\pi R/\lambda \qquad (1)$$
$$\phi_2 = 4(R + \Delta R)/\lambda$$
$$\Delta\phi = \phi_1 - \phi_2 = 4\pi\Delta R/\lambda$$

Where:

$\Delta\phi$	: DInSAR different phase between two SAR Image
ϕ_1 and ϕ_2	: is a phase of master and slave SAR images,
R	: is slant range and
λ	: is radar transmitting wavelength (C-band 5.5 cm).

The next step was to calculate the phase difference between two SAR Images (DInSAR). The parameters used to calculate the phase difference are earth curvature, topographic, surface deformation, atmospheric condition, and noise [24] (see equation 2):

$$\Delta\phi = \Delta\phi_{flat} + \Delta\phi_{height} + \Delta\phi_{disp} + \Delta\phi_{atm} + \Delta\phi_{noise} \qquad (2)$$

Where:

$\Delta\phi$	: DInSAR the differential interferometric
($\Delta\phi$ flat)	: is the flat earth phase that presents in the interferometric phase
($\Delta\phi$ height)	: is a contribution of topographic in the interferometric phase referred to DEM
($\Delta\phi$ disp)	: is the relative displacement of the target T to the reference point
($\Delta\phi$ atm)	: is an interferometric phase that is introduced by an atmospheric condition,
($\Delta\phi$ noise)	: is the noise introduced by temporal condition, different look angle, or scatters.

The initial result of the DInSAR analysis is a single image with ambiguous values in phase (π). Phase's single image value is not easy to recognize. This value must enter into the unwarping stage to obtain the absolute phase value [22] following the equation 3:

$$d_{LOS} = \frac{\lambda x\, d_{\varphi}}{4\pi\, \theta} \qquad (3)$$

Where

d_{LOS}	: is unwarping value,
θ	: is the incident angle in each pixel, and
λ	: is the wavelength.

The result of the unwarping process equation (3) is the absolute value in phase units. Then this value must be converted into meter [23] using the following equation:

$$\phi^{n}{}_{defo} = \frac{4\pi}{\lambda} dn = \frac{4\pi tn}{\lambda} vp + \mu NL \quad (4)$$

Where:

$\phi^{n}{}_{defo}$	: is the deformation phase,
λ	: is the carrier wavelength,
dn	: is the light of sight distance change of the target;
vp	: is the constant velocity;
tn	: is the temporal baseline, and
μN	: is the phase term due to a possible non-linear motion.

From processing phase absolute interferometric data using equation (4), the deformation value is obtained in the form of a displacement in meters unit.

Data Sampling

The strategy for determining data sampling is one of the most important factors for assessing a data or the development of a geographic data, so that it is able to represent the whole data or population [19]. This research used 100 purposive sample locations to detect monthly surface deformations (Figure 1). The samples distribution shows that most surface inflation occurred around the volcanic crater, while most surface deflation occurred on the valley's slopes. This study uses a purposive sampling method as it avoids information errors. According to Jacob and Sinha, InSAR technology has lower accuracy in dense vegetation area [25]. Thus, the selected samples were mostly in non-forested area. The cross-section on the map was also used to extract monthly deformation information from 2021 to 2022.

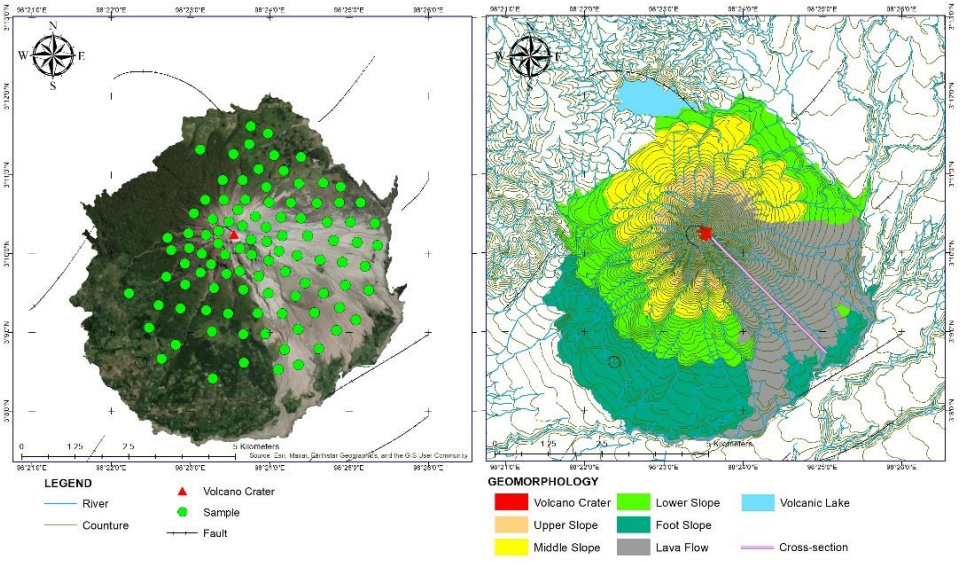

Figure 1. Sample distribution and cross section on the geomorphology map

RESULTS AND DISCUSSIONS

This study found a change the ground deformation every month from 2021 to 2022. Overall, the results of data processing by differential interferometry managed to provide displacement information in meter units, these values representing the time series of volcanic ground deformations. The sensitivity of the Sentinel-1 SAR satellite technology is able to detect detailed deformations of up to millimeter precision and cover the entire Mount Sinabung. The Radar capable of penetrating clouds and ash which is very efficient for monitoring mountains in various weather conditions [21]. The interferogram value is generated by cross-multiplying the master image by the standard of the equation. To reduce uncontrolled noise such as time, baseline and volume scattering in the interferogram, it is done by calculating the mean of neighboring pixels in a complex interferogram (multi-look) and applying active filtering (Goldstein filter). The variation of the interferometric values is proportional to the values of the two SARs divided by the transmitted wavelength [14]

The results of the interpretation of the SAR data showed ground surface movements that vary across the mountain and changes in the spatial distribution of deformations around the volcanic area. Some areas deflated while others inflated. From the monthly deformation map (see Figures 2 and 3), Mount Sinabung in 2021 experienced deformation rate with a range of values between 0.037 and -0.017 meters. This showed that Mount Sinabung inflation rate was greater than deflation rate. while the deformation occurred in 2022 has a maximum value of 0.042 meters to -0.040 meters.

There was inflation and deflation, which changed rapidly over a very narrow period of time, thus providing a very significant representation of changes in the volcano's physiographic surface. The spatial distribution pattern of this deformation tends to focus on the geomorphology of the crater, which is always under the endogenous pressure of the magma chamber that exerts pressure on the volcano's crater. The morphology of the volcanic cone is also very sensitive to this deformation. From the map it can be seen that the conical area of the volcano gives differences in the spatial distribution. It is shown by color information on deformation values, which are very contrasting in time series data.

From January to December 2022, the spatial distribution of inflation phenomenon concentrated on the morphology of the former eruption area or magma materials (southeast area of the crater), as well as the morphology of the foot slopes and central slopes of the volcano and the steep slopes around the crater (see Figure 2 and Figure 3). Meanwhile, deflation tended to occur only in the morphology of former eruptive materials on relatively gentle slopes. The morphological landscape of the former volcanic eruption has been deformed since the beginning of the observation period and this condition will persist until December 2022. In areas that have not undergone dramatic changes in deformation, the deformation will not appear as clearly in the subsequent period. The map also shows areas that have not undergone significant deformation, with a color symbol ranging from orange -0.003 meters to a purple color of 0.023 meters in 2021. The range of values and visualizations on this map are deformation phenomena that are not as contrasting as they've changed it since the month of data collection. This inflation can be caused by pressure from inside the volcano. The third is the phenomenon of volcanic deflation, which has a maximum range of values from -0.02 meters to -0.04 meters. This indicates a significant decrease in the volcano's surface area during the observation period of 2021-2022.

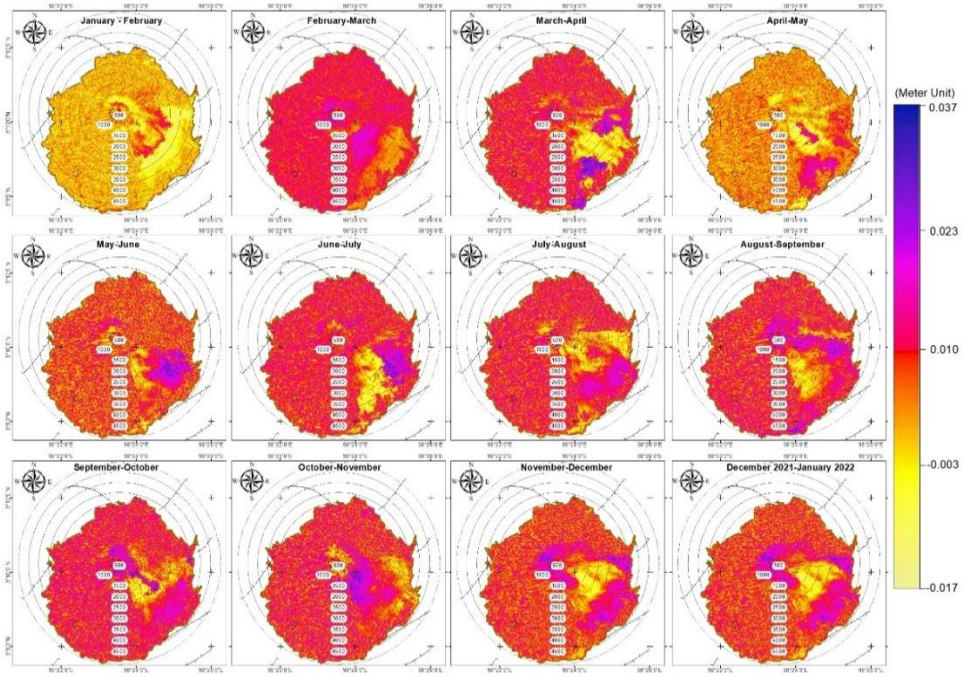

Figure 2. Volcano's surface deformation from January to December 2021

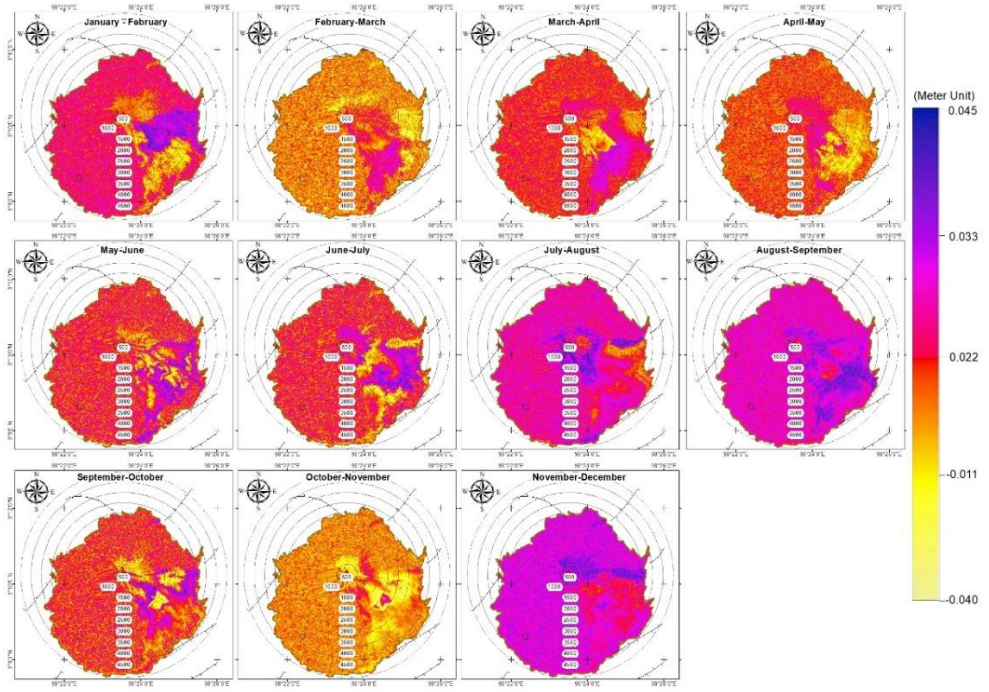

Figure 3. Volcano's surface deformation from January to December 2022

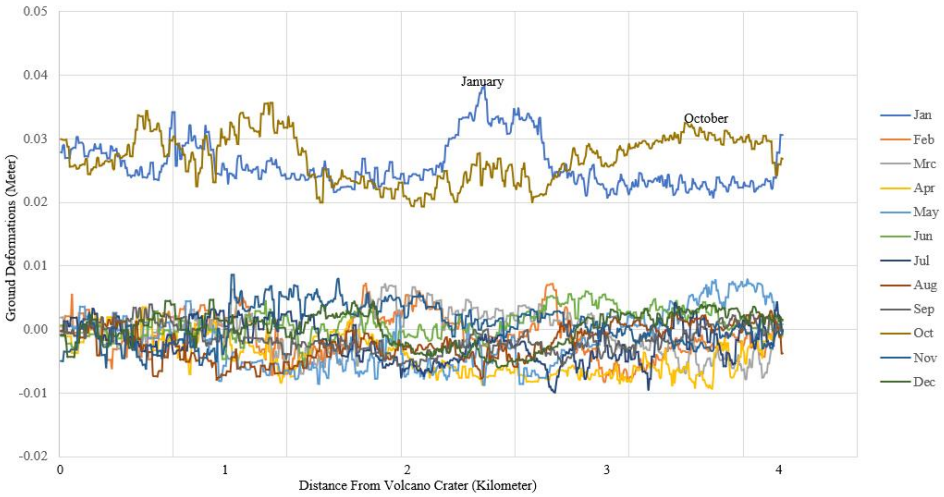

Figure 4. Cross section of Volcano's surface deformation from January to December 2021

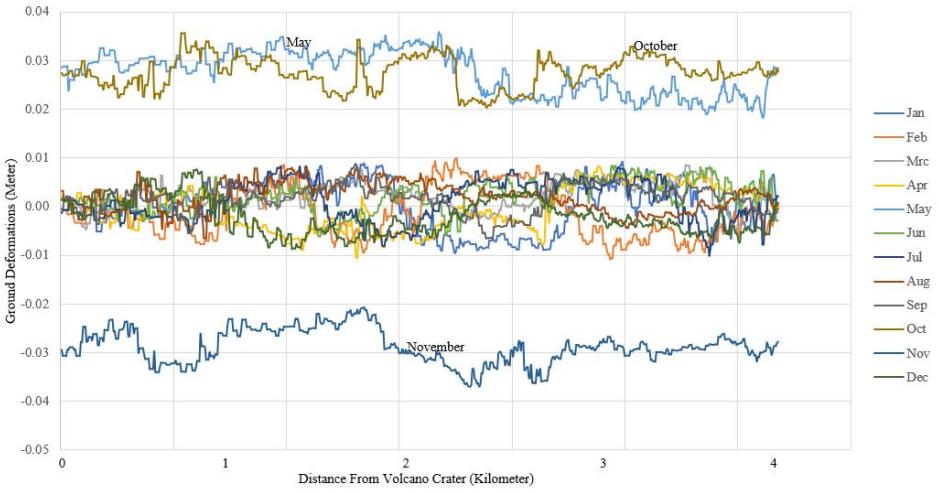

Figure 5. Cross section of Volcano's surface deformation from January to December 2022

This study performed a cross-section (Figures 4 and 5) to see changes in deformation each month from 2021 to 2022. It is emphasized that call as a normal position where there is no inflation or deflation, the position is at 0 meters means a stable point. While the shift in position from 0 to plus (inflation) or minus (deflation) is expressed as a form of land surface deformation. In the cross-sectional plot of Figure 4, it can be seen that the maximum level of deformation occurred in January and October 2021. This chart shows changes in inflation over the two periods, returning to its normal position. In this period, the deformation reached 0.03 meters, after which deformation still occurred, but it was not so different from conditions in other months. While in Figure 5 the deformation in 2022 shows different fluctuations, twice there was an inflation that was quite large, reaching a maximum value of about 0.035 meters, and a deflation that reached -0.035 meters from the normal position. This indicates that there is a contraction occurring in the magma chamber, causing significant pressure and shrinkage over a period of time. There significant deformation changes attributed to magma pressure activities from the Earth's interior causing inflation on the mountain surface. This is due to the increased magma pressure, which leads to changes in the volume of the mountain's surface, and over time shrinkage occurs, after which the mountain returns to its original position.

Zones that have undergone deformation are very unstable and brittle and become more susceptible to deformation at a later process [5]. It can be seen from the deformation map that the areas in the western and northern regions have not previously undergone dramatic changes and, unlike later periods, have not experienced any deformation activity. The deformation conditions are not only concentrated in the area around the crater, but in a radius of 4000 meters around the center of the crater of Mount Sinabung. The magma chamber continues to experience seismic activity, collapse and gas pressure, causing pressure fluctuations on the surface of the volcano, this phenomenon causes uplift in certain parts of the volcano and also causes magma intrusion [15]. The volcanic material and deformation to the southeast of the volcano has been evident since the 2010 and 2013 eruptions. The area was heavily damaged and covered with pyroclastic material. This was because the condition of the open slope area on this side of the volcano was very prone to deformation and landslides [11].

Figure 6 shows the monthly deformations that occurred. In March 2021 there were a total of 13 explosive eruptions that produced an ash cloud up to 5,000 m high. Incidentally, inflations of about 0.038 m were observed around the volcano a few months earlier. In addition, there were 26 eruptions in April 2021, with the largest eruption producing an ash plume of 1,600 m. From April to August, the deformation was about -0.01 to 0.01 meters. After another eruption in August 2021 with an ash plume height of 4,500 m, Sinabung volcano's deformation continued to experience inflation of about 0.038 m. There was drastic inflation in October, reaching 0.033 m and then falling dramatically to -0.037 m in November 2022. This indicated tectonic activity around the volcano caused by continuous changes in the underlying magma pressure.

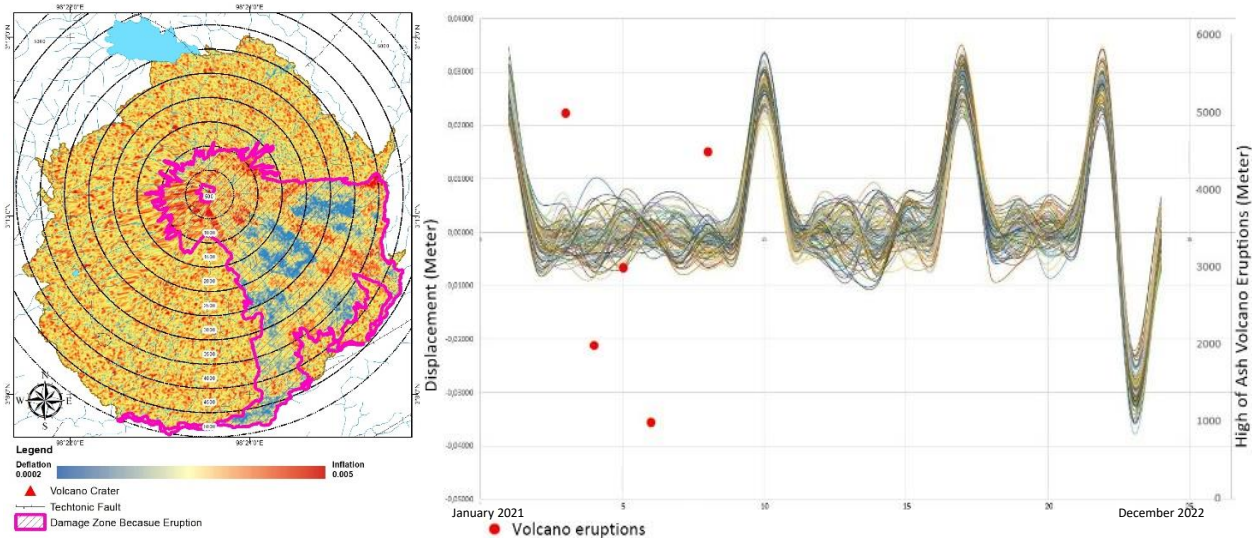

Figure 6. Map average deformation and surface deformation form January 2021 to December 2022.

From the observed results, it was clear that there were many drastic changes in strain at each sample location, whether or not an eruption had occurred. [3] Deformations that occurred in the environment can be caused by 2 scenarios. The surface could be deformed by an explosive eruption, or a new lava dome could

grow below the surface. Both scenarios need to be closely monitored as changes in the shape of the lava dome can also lead to eruptions [5].

The results of this study showed that the area with the highest occurrence of ground deformation were the southeast area of the crater where previous volcanic eruptive materials has been piled up. Although this displacement is small, the ground deformations has been occurring continuously and unstable (see Figure 6). Landslides can occur easily as this area is covered with young rocks resulting from eruption materials. Deformation has a significant impact on slope stability. Changes in slope geometry cause slopes to become steeper or flatter, which can lead to slope failure [16]. The frequent occurrence of ground deformations can also affect soil displacements and its stability [17]. The appearance of cracks, through which water can enter, can increase the water pressure on the embankment and lead to embankment failures. We found that two years of monthly deformation data were insufficient to unambiguously determine patterns, trends, and correlations between ground deformation and volcanic activity. Thus, more data is needed to perform a more accurate correlation and autocorrelation.

CONCLUSION

DInSAR technique is very efficient for monitoring the spatial deformation of volcanoes. Sinabung volcano is an active volcano, which experiences erratic inflation and deflation. Although there were no explosive eruptions in 2022, the volcano still experienced surface deformations caused by endogenous and exogenous forces affecting the morphological configuration or surface of the volcano. Surface deformation might not always lead to explosive eruptions, however, the energy continued to accumulate, and caused the volcano to erupt in February 2023, producing smoke from the crater around 500 m high. Thus, it is imperative to gather more data, to continue monitoring the volcano activity, and to analyze the autocorrelation between the deformation and eruption events. The result showed that the volcano is still very active and more eruptions are expected.

ACKNOWLEDGMENT

The authors would like to acknowledge the College of Computing Khon Kaen University for awarding the Active Recruitment Scholarship ARC 2022. To the ESA Copernicus online data centers for providing Sentinel 1 SAR Data.

REFERENCE

[1] Hendrasto M, et al. 2012. Evaluation of Volcanic Activity at Sinabung Volcano, After More Than 400 Years of Quiet. Journal of Disaster Research Vol.7 No.1. https://www.fujipress.jp/jdr/dr/dsstr000700010037/

[2] Magma Indonesia. 2023. Volcano Observatory Notice for Aviation. Center Vulcanology. Ministry Geology and Mineral Resorces. https://magma.esdm.go.id/v1/vona.

[3] Voaindonesia. 2021. Kerugian Akibat Erupsi Gunung Sinabung https://www.voaindonesia.com/a/kerugian-akibat-erupsi-sinabung-ditaksir-capai-rp-29-miliar-

[4] Lee Chang-Wook,Lu Zhong and Jin Woo Kim. 2017. Monitoring Sinabung volcano in Indonesia Using Multi-Temporal InSAR. Korean Journal of Remote Sensing, Vol.33, No.1, 2017, pp.37~46.

[5] Mulyaningsih Sri. 2015. Vulkanologi. Penerbit Ombak Press. Jl Progo B-15 Yogyakarta. ISBN: 978-602=258-322-6.

[6] Jerram Dougal. 2021. Introducing Volcanology a Guide to Hot Rock. Second Edition. Dunedin Academic Press Ltd, 8 Albany Street Edinburgh.

[7] Gatsios Theodoros, Cigna Francesca, Tapete Deodato, Vassilis Sakkas, Kyriaki Pavlou and Issaak Parcharidis. 2020. Copernicus Sentinel-1 MT-InSAR, GNSS and Seismic Monitoring of Deformation Patterns and Trends at the Methana Volcano, Greece. MDPI Journal Apply Science 10.

[8] Devanthéry Núria, Crosetto Michele, Monserrat Oriol, Cuevas-González María and Crippa Bruno. Deformation monitoring using Sentinel-1 SAR data. The 2nd International Electronic Conference on Remote Sensing (ECRS 2018), 22 March–5 April. Sciforum Electronic Conference Series, Vol. 2018

[9] Agram, P.S.;Warren, M.S.; Calef, M.T.; Arko, S.A. 2022. An Efficient Global Scale Sentinel-1 Radar Backscatter and Interferometric Processing System. Remote Sens. 2022, 14, 3524.

[10] Aditiya et al. Surface deformation monitoring of Sinabung volcano using multi temporal InSAR method and GIS analysis for affected area assessment. IOP Conf. Ser.: Mater. Sci. Eng. 2018. DOI 10.1088/1757-899X/344/1/012003

[11] Santi, P., Galderisi, A., Rastello, D., & Martino, S. 2015. Integrated landslide susceptibility assessment in the archaeological site of Pompeii (Italy). Bulletin of Engineering Geology and the Environment, 74(3), 771-786.
[12] Gatsios Theodoros, Cigna Francesca, Tapete Deodato, Vassilis Sakkas, Kyriaki Pavlou and Issaak Parcharidis. 2020. Copernicus Sentinel-1 MT-InSAR, GNSS and Seismic Monitoring of Deformation Patterns and Trends at the Methana Volcano, Greece. MDPI Journal Apply Science 10, 6445; https://doi:10.3390/app10186445.
[13] Duan Wei, et.al. 2020. Multi-Temporal InSAR Parallel Processing for Sentinel-1 Large-Scale Surface Deformation Mapping. MDPI. Journal Remote Sensing. doi:10.3390/rs12223749.
[14] A. Ferretti, A. Monti-Guarnieri, C. Prati, and F. Rocca, "InSAR processing: a practical approach," in ESA Publications, vol. B, 2007, pp. 1–40.
[15] Cashman, K. V., & Sparks, R. S. J. 2013. How volcanoes work: a 25 year perspective. Geological Society, London, Special Publications, 380(1), 1-27. GSA Bulletin (2013) 125 (5-6): 664–690. https://doi.org/10.1130/B30720.1
[16] Gudmundsson Agust. 2016.The mechanics of large volcanic eruptions. Earth-Science Reviews. Volume 163, December 2016, Pages 72-93 https://doi.org/10.1016/j.earscirev.2016.10.003
[17] Blundy Jon and Cashman Kathy. 2008. Petrologic reconstruction of Magmatic SystemVariables and Processes. Reviews in Mineralogy & Geochemistry Vol. 69 pp. 179-239, Mineralogical Society of America. DOI: 10.2138/rmg.2008.69.6
[18] Wu Shuo-sheng, et al. 2005. Population Estimation Methods in GIS and Remote Sensing; A Review. Department of Geography, Texas State University- San Marcos. Journal GIScience and Remote Sensing. 42. No. 1, p. 58-74.
[19] Zhang Jiping et al. 2013. Application of Spatial Sampling to Remote Sensing Monitoring of Forest Cover Area. Journal Advance Material Research Vol 610-613. Doi: 10.4028/www.scientific.net/AMR.610-613.3732.
[20] Haryanto Iyan. 2011. Struktur Geologi Pada Zona Transisi Antara Busur Volkanik Bukit Barisan Dengan Cekungan Belakang Busur : Contoh Di Daerah Sumatra Utara. Bulletin of Scientific Contribution, Volume 9, Nomor 1, April 2011: 8 -16. https://doi.org/10.24198/bsc%20geology.v9i1.8258.g3805.
[21] Kusky Timothy. 2008.Volcanoes: Eruptions and Other Volcanic Hazards. An imprint of Infobase Publishing 132 West 31st Street. New York NY 10001. ISBN-13: 978-0-8160-6463-2.
[22] Hanssen, R.F. 2001. Radar Interferometry. Data Interpretation and Error Analysis. Springer. Series Book Remote Sensing and Digital Image Processing. https://doi.org/10.1007/0-306-47633-9 .
[23] Minh Tong Ho Dinh,Ngo Yen-Nhi, Lê Trang Thu, Le Chon Trung, Bui Son Hong, Vuong Viet Quoc, Toan Le Thuy. 2020. Quantifying horizontal and vertical movements in Ho Chi Minh city by Sentinel-1 radar interferometry. Preprint. doi:10.20944/preprints202012.0382.v1.
[24] Razi Pahkrul et al. 2019. Ground deformation measurement of Mount Sinabungeruption using Din SAR technique. IOP Conference. Series: Journal of Physics: 1185 (2019) 012008. doi:10.1088/1742-6596/1185/1/012008.
[25] Alexander Jacob, Claudia Notarnicola, Gopika Suresh, Oleg Antropov, Shaojia Ge, et al. 2020. Sentinel1 InSAR Coherence for Land Cover Mapping: A Comparison of Multiple Feature-Based Classifiers. IEEE Journal of Selected Topics in Applied Earth Observations and Remote Sensing, 13, pp.535- 552. ff10.1109/JSTARS.2019.2958847ff. ffhal-02494546f
[26] Sinha Suman, Sharma K L,Jeganathan C, Nathawat M S, Anup K. DasV, and Mohan Shiv . 2015. Efficacy Of Insar Coherence In Tropical Forest Remote Sensing In Context Of Redd. International Journal of Advancement in Remote Sensing, GIS and Geography. IJARSGG (2015) Vol.3, No.1a, 38-46. ISSN 2321–835

View publication stats